Archives of Materials Science and Engineering

Volume 97
Issues 1-2
May-June 2019
Pages 20-38

International Scientific Journal
published monthly by the
World Academy of Materials
and Manufacturing Engineering

DOI: 10.5604/01.3001.0013.2869

Parametric characterization of a meso-mechanic kinematic in plain and twill weave 2/2 reinforced composites by FE-calculations

M. Romano [a], I. Ehrlich [a,*], N. Gebbeken [b]

[a] Laboratory of Composite Technology (LFT), Department of Mechanical Engineering, Ostbayerische Technische Hochschule Regensburg (OTH.R), Galgenbergstrasse 30, 93053 Regensburg, Germany

[b] Institute of Engineering Mechanics and Structural Analysis, Department of Civil Engineering and Environmental Sciences, University of the Bundeswehr Munich, Werner-Heisenberg-Weg 39, 85577 Neubiberg, Germany

* Corresponding e-mail address: ingo.ehrlich@oth-regensburg.de

ABSTRACT

Purpose: A parametric characterization of a mesomechanic kinematic caused by ondulation in fabric reinforced composites is investigated by numerical investigations.

Design/methodology/approach: Due to the definition of plain representative sequences of balanced plain-weave and twill-weave 2/2 fabric reinforced single layers based on sines the variable geometric parameters are the amplitude and the length of the ondulation.

Findings: The mesomechanic kinematic can be observed in the FE analyses for both kinds of fabric constructions.

Research limitations/implications: The FE analyses consider elasticity and contraction due to Poisson effects, respectively, of the model under selected longitudinal strains.

Practical implications: The results are evaluated at relevant positions on the centre-line of the ondulated warp-yarn of the plain representative model. A direct and linear coupling in case of the transversal kinematic behaviour, and thereby a corresponding definite reduction of the evaluated longitudinal strains in terms of the difference of the applied and determined longitudinal strains is identified.

Originality/value: Both characteristic purely kinematic reactions due to geometric constraints directly depend on the introduced degree of ondulation. This non-dimensional parameter relates amplitude and length of one complete ondulation, and thus represents the intensity of the ondulation of the respective fabric construction.

Keywords: Fibre reinforced plastics, Mesomechanic scale, Fabric reinforced layer, Ondulation

Reference to this paper should be given in the following way:

M. Romano, I. Ehrlich, N. Gebbeken, Parametric characterization of a mesomechanic kinematic in plain and twill weave 2/2 reinforced composites by FE-calculations, Archives of Materials Science and Engineering 97/1-2 (2019) 20-38.

METHODOLOGY OF RESEARCH, ANALYSIS AND MODELLING

1. Introduction

Simplified theoretical approaches for fibre reinforced plastics often presume a layup of only unidirectionally reinforced single layers. As a first approach in applied engineering the structural mechanic properties can analytically be determined by the use of so-called micromechanical homogenization theories. These are usually based on the single components' properties, namely matrix and fibre. However, different kinds of fabrics are often applied as reinforcements in the layup of structural parts. In this case homogenization theories reach their limit. The reason therefore is that the mesomechanic geometry of fabric reinforced single layers cannot be considered sufficiently by relatively simple homogenization approaches. Yet, mesomechanic correlations are distinctly different as they significantly influence the mechanical properties of a structure.

2. Research environment

Selected literature of the structural mechanic behaviour of fabric reinforced plastics is chronologically presented. The conclusions lead to the pursued mechanical principle.

2.1. Literature review

Naik and Shembekar [1] present linear-elastic investigations of plain-weave fabrics. Mital, Murthy and Chamis [2] investigate the micromechanics of plain weave composites. Guan [3] investigates the visco-elastic damping in fabrics. Byun [4] presents an analytical model of a mesomechanic unit cell. Huang [5] introduces a bridging model for the mechanical description of fabrics. Guan and Gibson [6] suppose the acting of a mesomechanic mechanism for damping in fabrics. Tabiei and Yi [7] confront different methods for the determination of material properties of fabrics. Le Page et al. [8] carry out two-dimensional FE calculations, presuming plane stress and considering mesomechanic parameters. Wielage et al. [9] emphasize the relevance of a detailed mesomechanic description of fabrics. Barbero et al. [10] present FE calculations of plain-weave fabrics in `in-' and `out-of-phase' arrangement. Ballhause [11] investigates the mesomechanics of dry fabrics under one- and two-dimensional loading. Matsuda et al. [12] presents a homogenization for elastic and visco-plastic parts in plain-weave fabrics. Nakanishi et al. [13] investigate the damping properties of fabrics. Badel, Vidal-Sallé and Boisse [14] as well as Hivet and Boisse [15] identify mesomechanics of dry fabrics under biaxial tension. El Mahi et al. [16] give an analytical description of the material damping in fabrics. Szablewski [17] considers representative sequences of plain-weave fabrics with sine-shaped ondulations. Hivet and Duong [18] carry out numerical investigations for dry fabrics under shear loading. Ansar, Xinwei and Chouwei [19] review modeling strategies of textile reinforced composites. Kreikmeier et al. [20] introduce in-plane sine-shaped fiber-orientation as imperfections obtained by a defined manufacturing process.

2.2. Pursued mechanical principle

Based on a sine according to equation (2) a plain representative sequence of a balanced plain-weave and twill-weave 2/2 fabric is derived. The amplitude A and the length L are the characteristic geometric parameters. The geometries for the FE analyses are shown in Figure 1, left of a plain-weave fabric and right of a twill-weave 2/2 fabric, both balanced.

The simplified geometry of the ondulation represents an idealized cross-section of the warp yarn of a fabric. The cured state of the composite material with a polymeric matrix system is considered. Three structural mechanically different regions, with locally orientated stiffnesses can be identified.

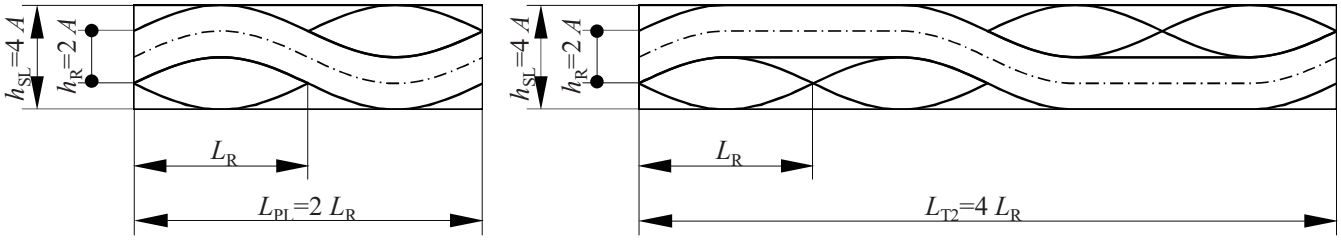

Fig. 1. Sequences of one full ondulation of a plain-weave (left) and twill-weave 2/2 fabric (right)

It is firstly the the warp yarn with predominant direction, i. e. E_1, following the longitudinal sine, and E_2 perpendicular to it. Secondly there are the fill yarns with predominant direction perpendicular to the cross-section, i. e. $E_2 = E_3$ in the plain model. Thirdly there is the matrix region that is not reinforced at all with E_m. The relations can mathematically be related by

$$E_1 >> E_2 > E_m \ . \tag{1}$$

Common homogenization theories yield $E_1 = 150$ GPa $>> E_2 = 11.5$ GPa $> E_m = 3.3$ GPa in case of a unidirectionally reinforced single layer with high tenacity (HT) carbon fibres with a presumed fibre volume content of $\varphi_f = 60$ % as absolute values for the stiffnesses. In relative terms it is $E_1 \approx 13 \cdot E_2$ and $E_1 \approx 45 \cdot E_m$, what respects the qualitative correlation (1).

The described structural mechanic relations cause a mesomechanic kinematic due to geometrical constraints only. Two different effects in the model can be identified, when positive and negative longitudinal deformations are considered. In both cases the unidirectionally reinforced ondulated yarn is subjected to a purely elastic deformation. Additionally at the same time in case of positive longitudinal deformations a smoothing or flattening, and in case of negative deformations an upsetting of the unidirectionally reinforced ondulated yarn is induced due to its ondulated shape. Thereby, the variation of the amplitude is a superposition of transversal deformation due to Poisson effects as an elastic response and a kinematic one due to mesomechanic constraints.

The repeated acting of this mesomechanic kinematic due to geometric constraints is presumed to enhance the damping properties of fabrics compared to unidirectionally reinforced ones. For an evaluation the free decay behaviour of flat beamlike specimens with fabric and unidirectional reinforcement can be considered. Thereby the fixed-free boundary condition has been identified as adequate. During the free decay the structure undergoes the kinematic in a number of cycles equal to the fundamental frequency.

The concept and the identification of the acting mechanism has been validated basically in Ottawa et al. 2012 [21] for one set of comparable specimens of basalt fibre reinforced epoxy (0° unidirectionally and 0° twill-weave 2/2 fabric reinforced in warp direction). There are even more detailed and validated investigations of Romano, Ehrlich and Gebbeken 2016 [22], Romano et al. 2014 [23],[24] and Romano 2016 [25] for three sets of comparable specimens of carbon fibre reinforced epoxy (0° unidirectionally and 0° plain and twill fabric 2/2 reinforced in warp direction).

3. Mesomechanic approach

The effect of ondulation is an effect on the mesoscopic scale in fabrics as textile semi-finished products. The number of ondulated yarns at one time depends on the type of fabric structure, and yields the characteristic pattern. In the following a plain-weave and a twill-weave 2/2 fabric, both balanced, are considered further.

The geometric parameters of the plain representative sequences are the amplitude A and the length of the ondulation in the fabric L_F or the one of the cross-section of a roving as a fill yarn L_R. The parametric variation in realistic steps provides the analysis of the sensitivity of the mesomechanic kinematic to the differently shaped ondulations.

3.1. Degree of ondulation

In order to definitely describe the differently shaped ondulations regarding the respective intensity of ondulation the specific value $\tilde{O}$ is introduced. The non-dimensional value is based on the afore mentioned characteristic and variable geometric parameters illustrated in in Figure 1. The definition of the degree of ondulation is based on an analytical sine

$$y = A \sin\left(2\pi \frac{x}{L}\right) \ . \tag{2}$$

For modeling more sequences in a row it can be repeated in series as often as required and still yields a continuously differentiable function over the whole domain of definition [26],[27]. For the introduction of the degree of ondulation $\tilde{O}$ the wave steepness used in nautics, as exemplarily defined in Büsching 2001 [28]

$$y = A \sin\left(2\pi \frac{x}{L}\right) \tag{3}$$

is modified. In equation (3) the geometric parameters are the (absolute) wave height $H = 2A$ and the wave length L. In contrast, following the outlook of Ottawa et al. 2012 [21] and the ideas described in Romano et al. 2014 [22], [23] and 2016 [24][25], the degree of ondulation in fabric reinforced plastics is defined by

$$\tilde{O} = \frac{A}{L} = \frac{A}{L_F} = \frac{A}{\lambda L_R} \ , \tag{4}$$

with the geometric parameters A, L_F and L_R, c. f. Figure 1, and λ as a characteristic factor for the type of the fabric. It is $\lambda = 2$ for a plain weave and $\lambda = 4$ for a twill weave 2/2

fabric. It can be varied for further different fabric constructions. In case of the considered ones it is

$$L_{PL} = \lambda L_R = 2 L_R = L_F \quad \text{and} \quad L_{T2} = \lambda L_R = 4 L_R = L_F \qquad (5)$$

3.2. Comparison of the structural mechanical motivations

The reason for the modification of the wave steepness S in equation (3) to the degree of ondulation $\tilde{O}$ in equation (4) is based on the different motivations, necessities and intentions of the respective subject area. In nautics it is important to characterize the absolute load a structure undergoes during its life-cycle, e.g. regarding fatigue strength issues. The considered structure is usually a ship on two supports. Thereby, it is necessary to evaluate the free carrying length of the ship structure relatively to the wave length L and the wave height H. Therefore, twice the amplitude A as the absolute wave height H is considered in the calculation of the specific value S [28].

In contrast, when fabric reinforced composites are considered, the characterization of the deviation from the ideally orientated unidirectionally reinforced single layer caused by the ondulation in the fabric is focused [29]. The modification towards considering the single value of the amplitude A can also be interpreted as a degree of eccentricity compared to an unidirectionally reinforced single layer that exhibits an ideally orientated reinforcement without ondulations. The height H of the ondulation $\tilde{O}$ corresponds to the amount of differing orientated fibre longitudinal directions. As a weakening of the structure it represents the tendency to additional relative deformations under loading, i.e. resulting damping is induced.

The degree of ondulation enables the comparability of the models and the numerical investigations. This is at the same time the requirement for a verification. The geometric dimensions are chosen in selected and at the same time realistic steps. The amplitude A is varied from 0.05 mm to 0.25 mm and the length of the cross-section of a roving L_R from 2.5 mm to 7.5 mm, each parameter in five substeps. According to equation (5) this yields lengths of the ondulation for a plain-weave fabric L_{PL} from 5.0 mm to 15.0 mm and for a twill-weave 2/2 fabric L_{T2} from 10.0 mm to 30.0 mm.

The selected values can be considered realistic, as described in detail for the comparable sets of specimens in the experimental validations carried out in Ottawa et al. 2012 [21] and in Romano et al. 2014 [22],[23] and 2016 [24],[25] or reported by Ballhause 2007 [11], Matsuda et al. 2007 [12] and Kreikmeier et al. 2011 [20].

According to equations (4) and (5) the afore listed geometric parameters yield values of the degree of ondulation $\tilde{O}$ for a plain weave fabric with $\lambda = 2$ lying in the range of 0.00333 and 0.05000 and for a twill-weave 2/2 fabric with $\lambda = 4$ lying in the range of 0.00166 and 0.02500, and it is $\tilde{O}_{PL} = 2\tilde{O}_{T2}$. Figure 2 illustrates the degree of ondulation $\tilde{O}$ over a plane spanned by amplitude A and length L of an ondulation, i.e. L_{PL} fand L_{T2} according to equation (5).

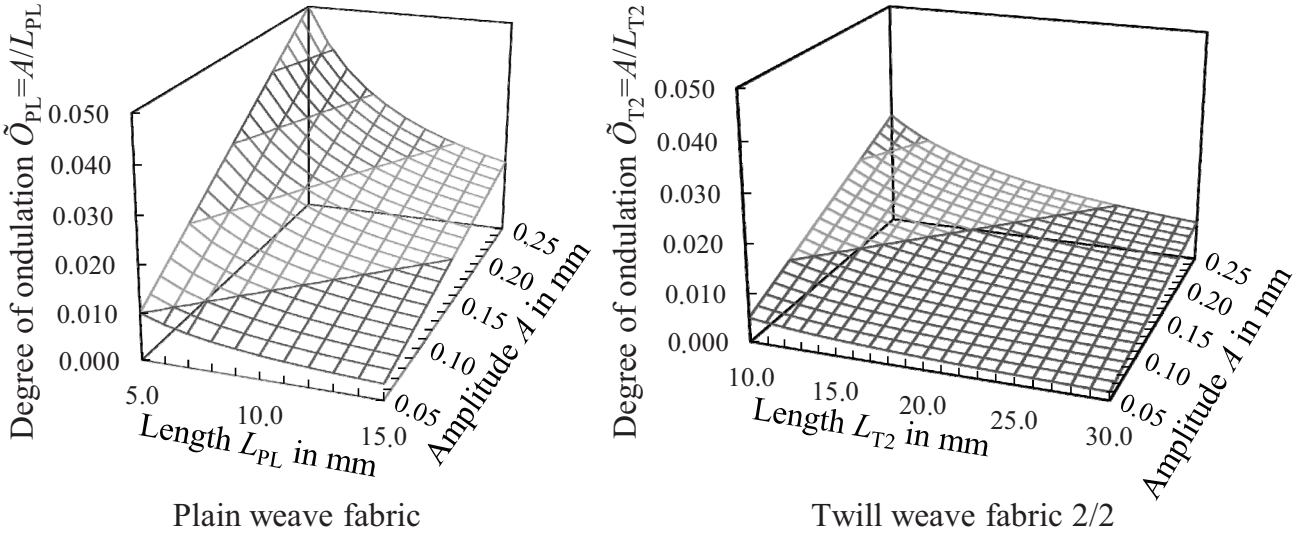

Fig. 2. Degree of ondulation $\tilde{O}$ over the geometric parameters

4. Numerical investigations by finite element analyses (FEA)

The selected variation of the geometric parameters enables the identification of the sensitivity of the mesomechanic kinematic concerning the intensity of the ondulation. As the FE calculations are linear-elastic analyses, elasticity and transversal deformation due to Poisson effects are present in the model. In order to identify the basically acting mesomechanic kinematic, correlations due to geometric constraints, non-linearities, failure mechanisms and friction effects are neglected. The modelling, setting and processing used, is based on the investigations of Ottawa et al. 2012 [21]. Therein different element formulations, number of elements (degree of discretization) and convergence behaviour is considered in sensitivity analyses. The FE software is ANSYS Workbench Version 14.0.1 [30].

4.1. FE model of plain representative sequences

In order to enable a proper meshing, avoid too small or acute triangle elements, reduce computing time and improve convergence the geometry is slightly modified. First, the lens-shaped fill yarns are cut by 2 % regarding the length L_R, yielding $L_{R,mod} = 0.96 \cdot L_R$. Second, the two horizontal boundaries are symmetrically moved outwards by 10 % of the amplitude A, in order to achieve a connected region of the matrix on top and bottom of the sequence. The resulting thickness of the modified sequences is then $t_{mod} = 4.2 \cdot A$. Figure 3 confronts the parametric models in the extremes of its geometric dimensions.

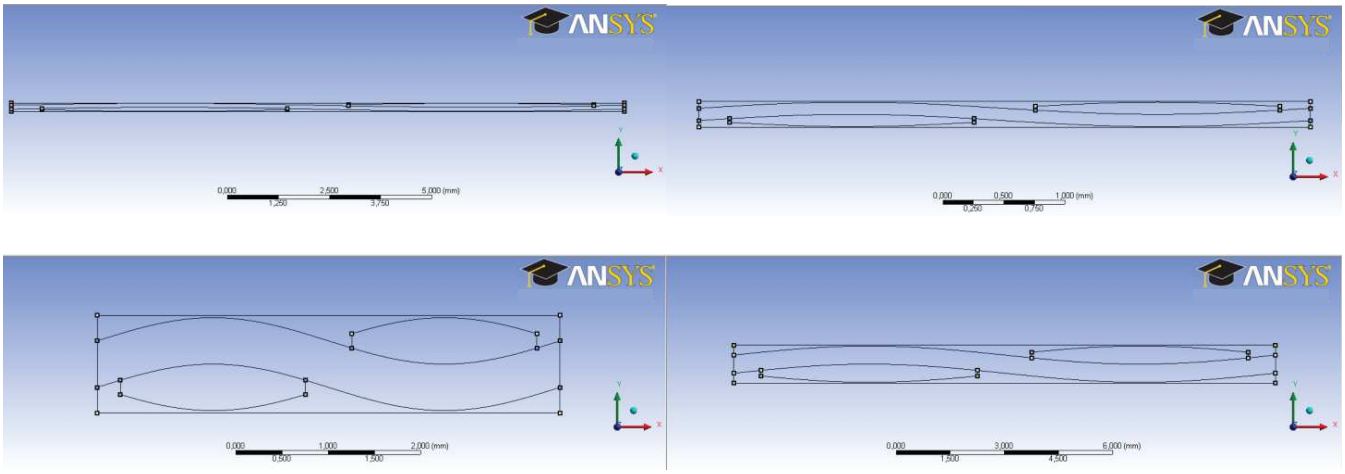

Fig. 3. Geometric extremes of the parametric FE-models: Top left: Biggest length/lowest amplitude; Top right: Shortest length/lowest amplitude; Bottom left: Shortest length/highest amplitude; Bottom right: Biggest length/highest amplitude

4.2. FE settings: meshing, element types and contact definition

A two dimensional FE analyses is carried out. The representative sequence is discretized by elements with an average edge length of $1 \cdot 10^{-3}$ mm. As the FE model represents a cross-section of a structure, a plain strain condition in the x-y-plane is presumed. Plain four-node shell elements are assigned. An orthotropic material model is chosen for properly applying the material properties to warp and fill yarn.

To the region of the warp yarn elements of the formulation PLANE42 are assigned to by APDL (ANSYS Parametric Design Language). The enabled first key option makes the local x-y-element coordinate system follow the element I-J-sides [30]. As a mapped meshing has been applied, the element coordinate systems, and so the properties of orthotropic materials, follow the sine-shaped ondulation.

For both other regions the default formulation PLANE182 are retained. A modification is not necessary, because the fill yarns are modelled transversally to their fibre longitudinal direction with isotropic material properties and the matrix is modelled full isotropic. The interaction between the single regions is defined by coincident matched nodes.

Figure 4 illustrates the effect of the different element formulations on the orientation of the element coordinate systems in the region of the zero-crossing.

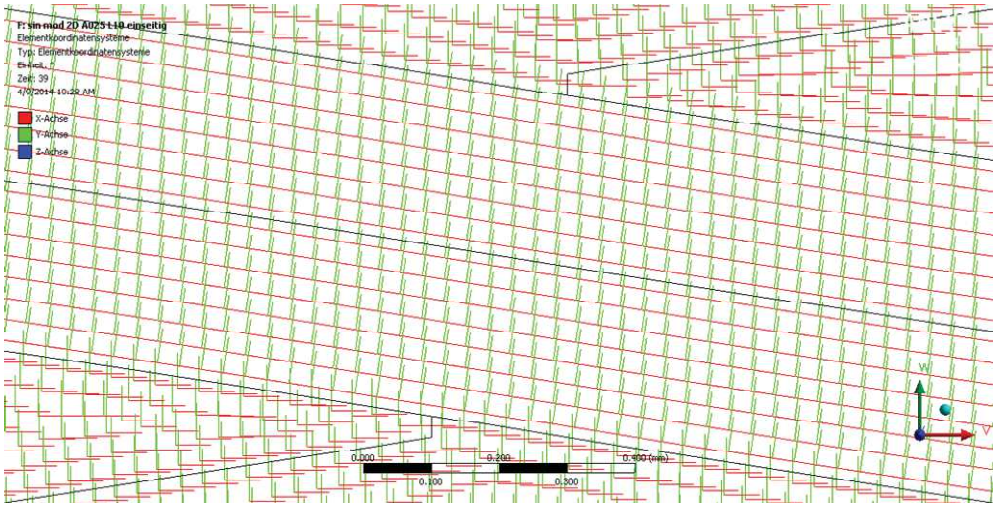

Fig. 4. Local element coordinate systems for element PLANE42 for the warp yarn and PLANE182 for fill yarns and matrix

4.3. Boundary conditions and application of selected deformations

A fixed edge is defined on one vertical edge. On the opposite vertical edge a free edge is defined, where the selected displacements are applied. Both definitions on the boundaries allow a transversal deformation of the cross-section due to Poisson effects. On the nodes of the defined free vertical edge selected longitudinal deformations as strains

$$\varepsilon_x = \frac{\Delta l}{l_0} = \frac{\hat{u}}{L_F} \tag{6}$$

in terms of relative displacements are applied. They have been selected in relevant ranges for fibre reinforced plastics [10],[29],[31]-[33]. Two decades are considered. The large interval is $\varepsilon_x = -1\cdot10^{-3} \ldots +1\cdot10^{-3}$ in steps of $1\cdot10^{-4}$ and the small one is $\varepsilon_x = -1\cdot10^{-4} \ldots +1\cdot10^{-4}$ in steps of $1\cdot10^{-5}$, i.e. 39 substeps.

Regarding the boundary conditions on the horizontal edges, i.e. on the top and bottom side of the model, two basically different conditions exist. Composites usually consist of more than one layer, mostly an even number of plies. The single layers can be considered as elastically supported on both sides, when located as an inner ply, and elastically supported on one side only, when located as an outer ply. Therefore, a case-by-case analysis is considered. The elastic support k_{el} represents a stiffness per unit length, where $[k_{el}] = \mathrm{N/mm^2} = \mathrm{MPa}$. The calculation of k_{el} is done by means of a weighted average of the plane stiffnesses E_2 and E_m based on the areas of the different regions, analogue to Barbero 2011 [38], 2006 [10] and 1995 [39] as well as to Byun 2000 [4].

4.4. Structural mechanic material properties of the single components

The two exemplarily considered single components are HT carbon fibres and epoxy resin, as commonly used in mechanically highly loaded structures. Table 1 contains the structural mechanic material properties [29],[31]-[33]. The indexing follows the principle of cause and effect, used usually in engineering sciences. Thus the Poisson's ratio $\nu_{ij} = -\varepsilon_j / \varepsilon_i$ represents the negative relation of the resulting deformation in j-direction due to an applied deformation in i-direction.

The densities of the single components as a physical material property are indicated for the HT carbon fibres $\rho_{\mathrm{HT-Carbon}} = 1.74\ \mathrm{g/cm^3}$ and for the epoxy resin system $\rho_m = 1.20\ \mathrm{g/cm^3}$. The material properties correspond to the values indicated in the data sheets of the three sets of comparable specimens, used in the experimental investigations described in Romano et al. 2014 [22],[23] and 2016 [24],[25].

4.5. Homogenized structural mechanic material properties

The fibre reinforced regions (warp and fill yarn) are considered as 0°-unidirectionally at the same local fibre volume content. The rovings have transversally isotropic material behaviour along the fibre direction. Thus, there are five independent structural mechanic material properties in the local 1-2-3-coordinate system.

Table 1.
Structural mechanic material properties of the single components [29],[31]-[33]

Reinforcement fibers	**HT Carbon**	**Polymeric matrix**	**Epoxy resin**
Structural mechanic material property	*Value*	*Structural mechanic material property*	*Value*
Young's modulus $E_{f,1}$	230 GPa	Young's modulus E_m	3.3 GPa
Young's modulus $E_{f,2}$	28 GPa	Shear modulus G_m*	1.22 GPa*
Shear modulus $G_{f,12}$	50 GPa	Poisson's ratio ν_m	0.35
Shear modulus $G_{f,23}$*	11.4 GPa*		
Poisson's ratio $\nu_{f,12}$	0.230		
Poisson's ratio $\nu_{f,21}$**	0.028**		
Poisson's ratio $\nu_{f,23}$	0.225		

* no independent material property, determined by $E = 2(1+\nu)G$ because of presumed (quasi-)isotropy

** no independent structural mechanic material property, determined by relation according to Maxwell-Betti

Table 2.
Homogenized structural mechanic material properties of the rovings of HT carbon fibre reinforced epoxy at the fibre volume content $\varphi_{f,R} = 65\ \%$ as the input values for the FE preprocessor of ANSYS [30]

Kind of fiber reinforcement		**HT carbon fiber reinforced epoxy**	
Region of plane rep. sequence	*Longitudinally cut (warp yarn)*	*Micromechanic homogenization*	*Transversally cut (fill yarn)*
Young's modulus E_1	150.7 GPa	weighted average stiff	11.4 GPa
Young's modulus E_2	11.4 GPa	Chamis 1983/84 [34],[35]	11.4 GPa
Young's modulus E_3	11.4 GPa	Chamis 1983/84 [34],[35]	150.7 GPa
Shear modulus G_{12}	5.7 GPa	Chamis 1983/84 [34],[35]	3.7 GPa*
Shear modulus G_{23}	3.7 GPa*	Tsai 1980 [36]	5.7 GPa
Shear modulus G_{13}	5.7 GPa	Chamis 1983/84 [34],[35]	5.7 GPa
Poisson's ratio ν_{12}	0.272	weighted average Poisson	0.333
Poisson's ratio ν_{23}	0.333	Foye 1972 [37]	0.021*
Poisson's ratio ν_{13}	0.272	weighted average Poisson	0.021*

* no independent structural mechanic material property for transversally isotropic material behaviour

Table 2 contains the homogenized structural mechanic material properties of the rovings, presumed as 0°-uni-directionally reinforced. They are indicated in the local 1-2-3-coordinate system of the respective region of the warp and fill yarn. Thereby, an achievable and technically reasonable local fibre volume content of the roving of $\varphi_{f,R} = 65\ \%$ is presumed. The density of the composite material ρ_c calculated as a weighted average of the densities of the single components based on the fibre volume content yields $\rho_{c,HT-Carbon-EP} = 1.55\ g/cm^3$.

The analytically determined global values of the representative sequence are for the fibre volume content $\varphi_{f,PRS} = 53\ \%$ and for the density $\rho_{PRS,HT-Carbon-EP} = 1.49\ g/cm^3$. However, the experimentally determined values of the test panels of the specimens used in in Romano et al. 2014 [22],[23] and 2016 [24],[25] are $\varphi_f \approx 59\ \%$ and $\rho_{HT-Carbon-EP} = 1.52\ g/cm^3$. The reasons arise due to the theoretical presumption of the plane representative sequence, that implies the so-called "in-phase" arrangement of subsequent layers. In contrast in reality the so-called "out-of-phase" arrangement occurs much more often, where huge conglomerations of pure matrix are very rare. Thus the fibre volume content and density of fabric reinforced layups are always closer to the "out-of-phase" arrangement, and slightly higher than the predicted by plane representative sequences. This fact is discussed in detail in Romano 2016 [22],[25].

4.6. Assignment of the structural mechanic material properties

To the fibre reinforced regions an orthotropic material behaviour is assigned. The input of three-dimensional properties is required, although two-dimensional ones are applied in the FE analyses [30]. Nine, usually independent, structural mechanic material properties are required. The pairwise equal input of the five independent values of the 0°-unidirectionally reinforced represents the existent transversal isotropic material behaviour, as indicated in. Table 2. To the regions of pure are assigned the isotropic material properties $E_m = 3.3\,\text{GPa}$ and $\nu_m = 0.35$ as indicated in Table 1. According to the case-by-case analysis, considering the two basically different boundary conditions, introduced in section 4.3, the calculated elastic support acting in transversal *y*-direction of the FE model is $k_{\text{el,HT-carbon-EP}} \approx 9.5\,\text{GPa}$. The detailed calculation of the elastic support k_{el} is done according to Barbero 2011 [38], 2006 [10] and 1995 [39] as well as to Byun 2000 [4].

5. Results

The evaluation of the results, the identified kinematic and its sensitivity to geometric parameters and boundary conditions are described.

Figures 6 to 9 illustrate the evaluated results, as described in the following. Because of better readability and overview they are placed at the end of section 5 in chronological appearance.

5.1. Aspects of the evaluation of the results

The results are evaluated for every degree of ondulation $\tilde{O}$ at every substep $n = 0,\ldots,39$ and plotted against the deformations ε_x (6). Thereby a linear correlation between the applied displacements and the considered relevant values is presumed, analogue to Ottawa et al. 2012 [21] and Romano 2016 [22],[25]. In detail the kinematic parts $\varepsilon_{y,\text{kin}}$ (9) and the difference of longitudinal deformations $\varepsilon_{x,\text{kin}}$ (12), as described in the following sections 5.3. and 5.4, are evaluated.

Sensitivity to the mesomechanic kinematic

Almost linear correlations can be identified, especially in the smaller interval. A direct and linear coupling between strain and shape of the ondulation can be stated. The absolute value of the slope as a function of the degree of ondulation

$$\tilde{M}_y\left(\tilde{O}\right) = \frac{\mathrm{d}\varepsilon_{y,\text{kin}}}{\mathrm{d}\varepsilon_x} \quad \text{and} \quad \tilde{M}_x\left(\tilde{O}\right) = \frac{\mathrm{d}\varepsilon_{x,\text{kin}}}{\mathrm{d}\varepsilon_x} \tag{7}$$

represents the sensitivity to the mesomechanic kinematic. The introduction of the slopes $\tilde{M}$ (7) defines another relative value. Thereby, a higher slope $\tilde{M}$ corresponds to a higher sensitivity to the mesomechanic kinematic.

Elastic and kinematic parts of the deformation behaviour

In the FE calculations the resulting deformation consists of the purely kinematic part due to geometric constraints and of the resulting elastic part of the linear-elastically modelled material. These two parts have to be separated from each other.

5.2. Positions of evaluation

The relevant positions of evaluation of the FE model are on the theoretical centre line of the ondulated warp yarn, as illustrated in Figure 5. In case of a plain weave fabric they are the two extrema. In case of the twill-weave 2/2 fabric they are the four positions at the transition of ondulated and horizontal regions and the two positions in the middle of the horizontal regions. At these positions the displacements in transversal direction (*y*-displacements *v*) and the longitudinal deformations (*x*-strains ε_x) are evaluated.

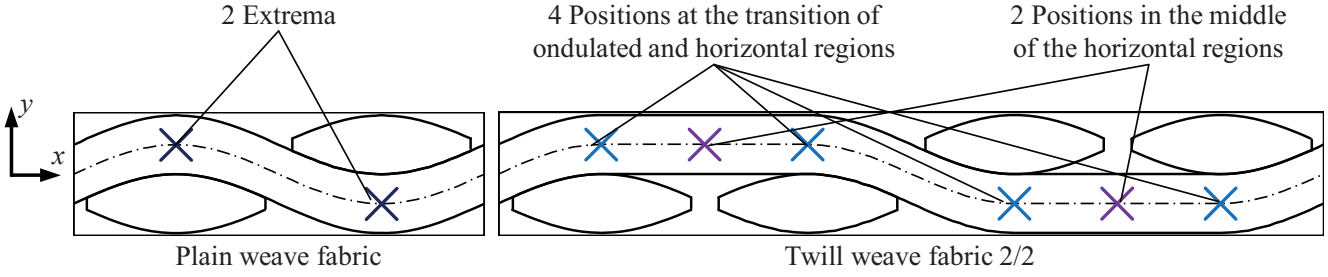

Fig. 5. Positions of evaluation of the plain representative sequences

5.3. Transversal kinematic part

The y-displacements v in transversal direction are evaluated by the difference of the values v_1 and v_2, where the indices indicate the opposite positions. The relative shift of the amplitude is the ratio of the difference of the y-displacements Δv to the originally perpendicular distance $2A$. The total transversal deformation is

$$\varepsilon_{y,n,\mathrm{tot}} = \frac{\Delta v}{2A} = \frac{v_{1,n} - v_{2,n}}{2A} \quad . \tag{8}$$

It is the sum of the purely kinematic part $\varepsilon_{y,\mathrm{kin}}$ as upsetting and flattening of the ondulated fibre, and the transversal strain $\varepsilon_{y,\mathrm{PRS}}$ due to Poisson's effects, i.e. contraction and dilatation of the sequence. These results (8) have to be corrected by the transversal deformation due to Poisson effects. Solved for the kinematic part it is

$$\varepsilon_{y,n,\mathrm{kin}} = \varepsilon_{y,n,\mathrm{tot}} - \varepsilon_{y,n,\mathrm{PRS}} = \frac{v_{1,n} - v_{2,n}}{2A} - \varepsilon_{y,n,\mathrm{PRS}} \quad , \tag{9}$$

where the transversal deformation due to Poisson effects is determined by

$$\varepsilon_{y,n,\mathrm{PRS}} = -\nu_{\mathrm{PRS},12}\, \varepsilon_{x,n} = -\nu_{\mathrm{PRS},12}\, \hat{u} \quad . \tag{10}$$

It is defined as the negative relation of transversal deformation due to the longitudinal one (cf. equation (6). The value $\nu_{\mathrm{PRS},12}$, used in equation (10), is calculated by the weighted average of the Poisson's ratios of the three regions based on its areas. It follows by

$$\nu_{\mathrm{PRS},12} = \frac{A_{\mathrm{W}}}{A_{\mathrm{PRS}}}\nu_{12} + \frac{A_{\mathrm{F}}}{A_{\mathrm{PRS}}}\nu_{23} + \frac{A_{\mathrm{M}}}{A_{\mathrm{PRS}}}\nu_{\mathrm{m}} \quad . \tag{11}$$

In case of the values of the HT carbon fibre reinforced epoxy, namely $\nu_{12} = 0.272$, $\nu_{23} = 0.333$ and $\nu_{\mathrm{m}} = 0.35$, as indicated in Table 1 and Table 2, equation (11) yields $\nu_{\mathrm{PRS},12} \approx 0.306$ as the value of the Poisson's ratio of the representative sequence.

5.4. Difference of applied and evaluated longitudinal deformation

An additional indicator for the acting of the mesomechanic kinematic due to geometric constraints is the difference of applied and evaluated deformations in longitudinal direction (x-direction) $\Delta\varepsilon_x = \varepsilon_{x,\mathrm{kin}}$. It is

$$\varepsilon_{x,n,\mathrm{kin}} = \Delta\varepsilon_{x,n} = \varepsilon_{x,n} - \varepsilon_{x,n,\mathrm{FE}} \quad . \tag{12}$$

The value is an indicator of the elastic deformation of the plain representative sequence and the ondulated warp yarn in the FE model.

5.5. Details of the sensitivity on the mesomechanic kinematic

The kinematic part $\varepsilon_{y,\mathrm{kin}}$ (9) plotted against the applied deformations ε_x always yields negative slopes. As described in section 2.2 positive deformations $\varepsilon_x > 0$ cause a flattening, and negative ones $\varepsilon_x < 0$ cause an upsetting.

The difference of longitudinal deformations $\varepsilon_{x,\mathrm{kin}}$ (12) plotted against the applied deformations ε_x always yields positive slopes $\tilde{M}$. The applied longitudinal displacements ε_x slightly differ from the evaluated ones. Thus, the acting of the mesomechanic kinematic reduces the resulting longitudinal deformation of the ondulated yarn. Additionally, in ranges of small deformations fabric reinforced composites nominally exhibit slightly lower stiffnesses as a 0°-unidirectionally reinforced sequence at a comparable fibre volume content. A similar tendency has been reported by Valentino et al. 2013 [40], 2014 [41] and Romano 2016 [22],[25], where basalt fibre reinforced plastics with different fabric reinforcements have been mechanically characterized by experimental tensile tests and FE calculations.

5.6. Results of the FE calculations

In case of the two-sided elastic support the opposed positions in the transversal y-direction behave symmetrically and contrary identical. In case of the one-sided elastic support the free position behaves distinctly more sensitive as the supported one. The results of the longitudinal x-direction behave identically in both cases.

The results of the plain-weave fabric are illustrated in Figure 6 for the kinematic parts $\varepsilon_{y,\mathrm{kin}}$ (9), and in Figure 7 for the difference of longitudinal deformations $\varepsilon_{x,\mathrm{kin}}$ (12). The results of the twill weave 2/2 fabric are illustrated in Figure 8 and 9 analogue.

Plain-weave fabric

With an increasing degree of ondulation the results show an increasing sensitivity. In case of the kinematic parts $\varepsilon_{y,\mathrm{kin}}$ (9) illustrated in Figure 6, it is possible to imply a sinusoid correlation. The case of the one-sided elastic support shows a 1.8 times higher sensitivity to the mesomechanic kinematic as the case of the two-sided one.

In case of the difference longitudinal deformation $\varepsilon_{x,\mathrm{kin}}$ (12) illustrated in Figure 7, it is possible to imply a quadratic correlation, where the one-sided elastic support shows again a higher sensitivity as the two-sided one.

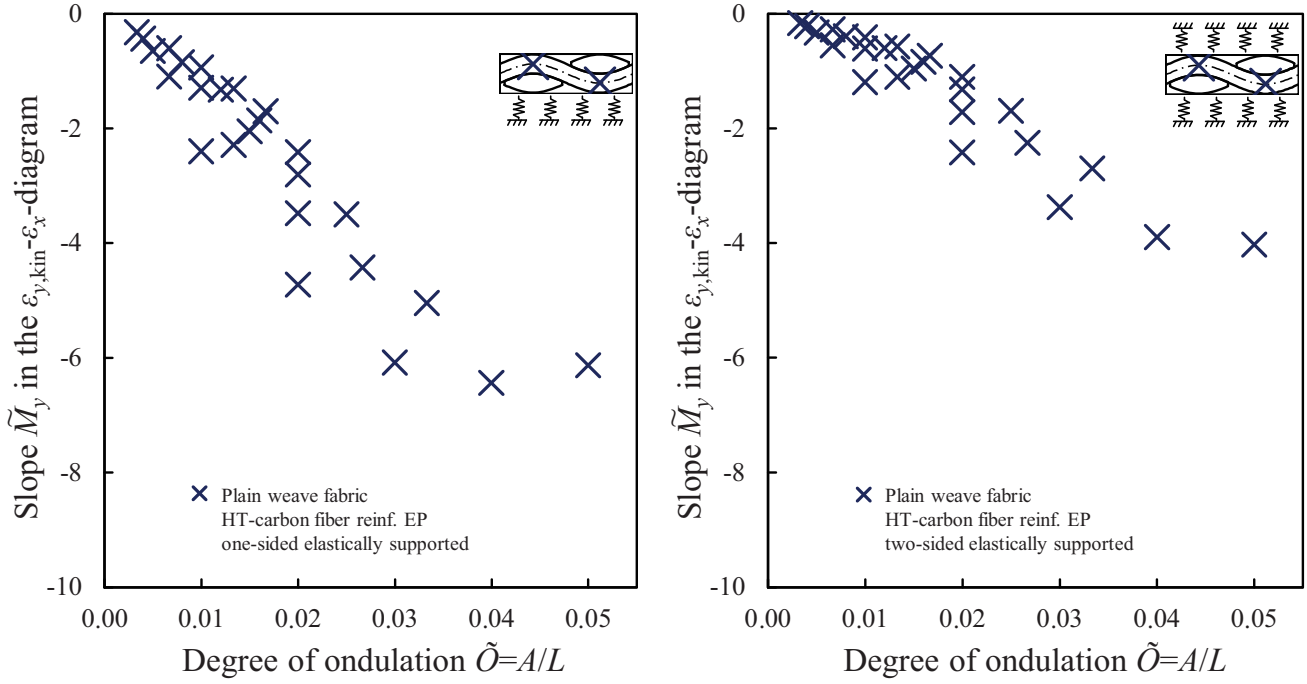

Fig. 6. Sensitivity $\tilde{M}_y(\tilde{O})$ of the transversal kinematic part $\varepsilon_{y,\mathrm{kin}}$ for plain-weave fabric

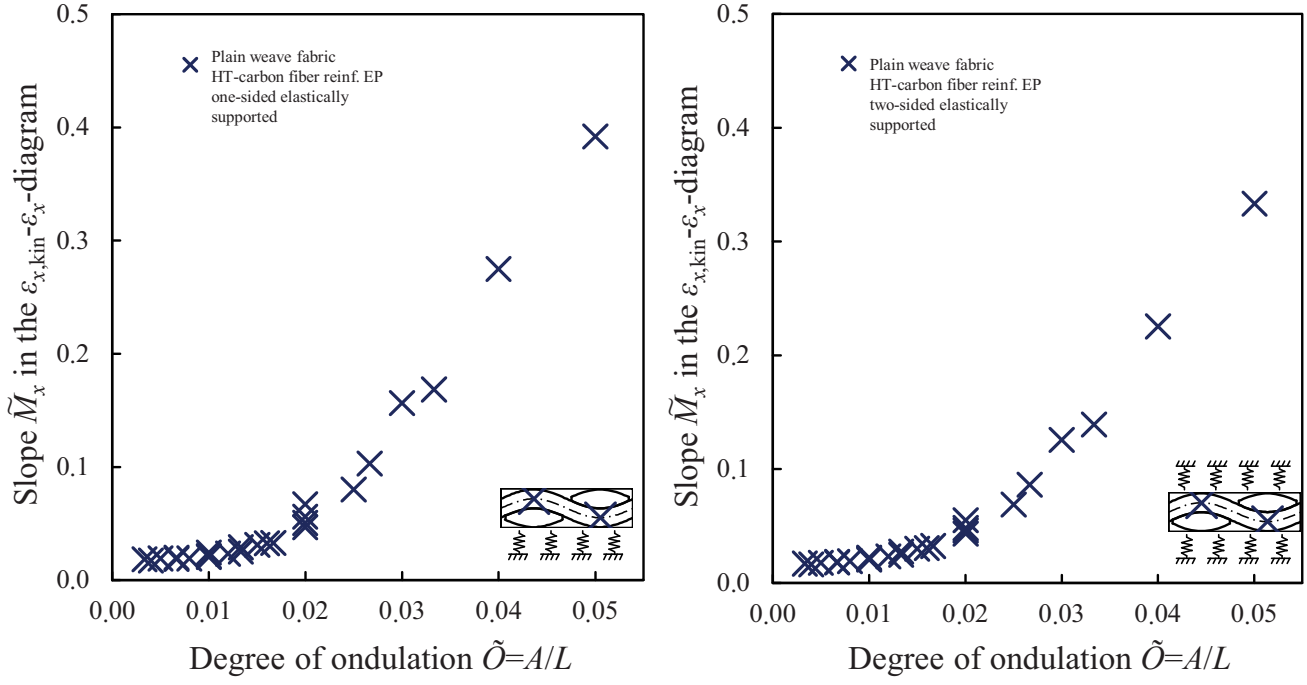

Fig. 7. Sensitivity $\tilde{M}_x(\tilde{O})$ of the difference of longitudinal deformation $\varepsilon_{x,\mathrm{kin}}$ for plain-weave fabric

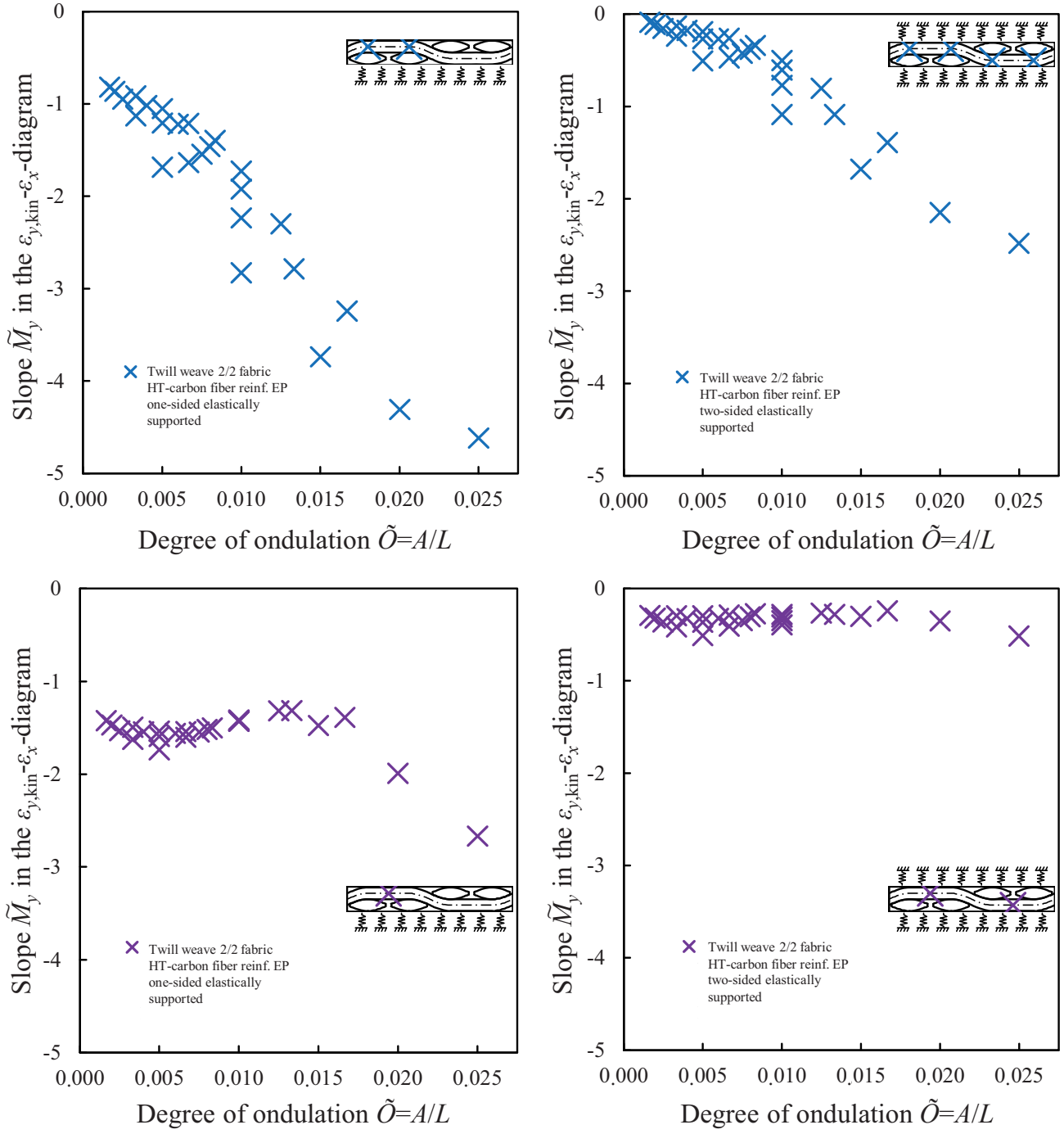

Fig. 8. Sensitivity $\tilde{M}_y(\tilde{O})$ of the transversal kinematic part $\varepsilon_{y,\mathrm{kin}}$ for twill-weave 2/2 fabric

Twill-weave 2/2 fabric

The positions of the transition of ondulated and horizontal regions show with an increasing degree of ondulation an increasing sensitivity, as illustrated in Figure 8. At these positions of evaluation it is once again possible to imply a sinusoid correlation in case of the kinematic parts $\varepsilon_{y,\mathrm{kin}}$ (9). Thereby, the case of the one-sided elastic support shows a 1.6 times higher

sensitivity to the mesomechanic kinematic as the case of the two-sided one. In contrast the two positions in the middle of the horizontal regions do not distinctly show the afore identified tendency at higher degrees of ondulation. The sensitivity of the kinematic parts $\varepsilon_{y,\mathrm{kin}}$ (9), especially in case of the two-sided elastic support, is very low.

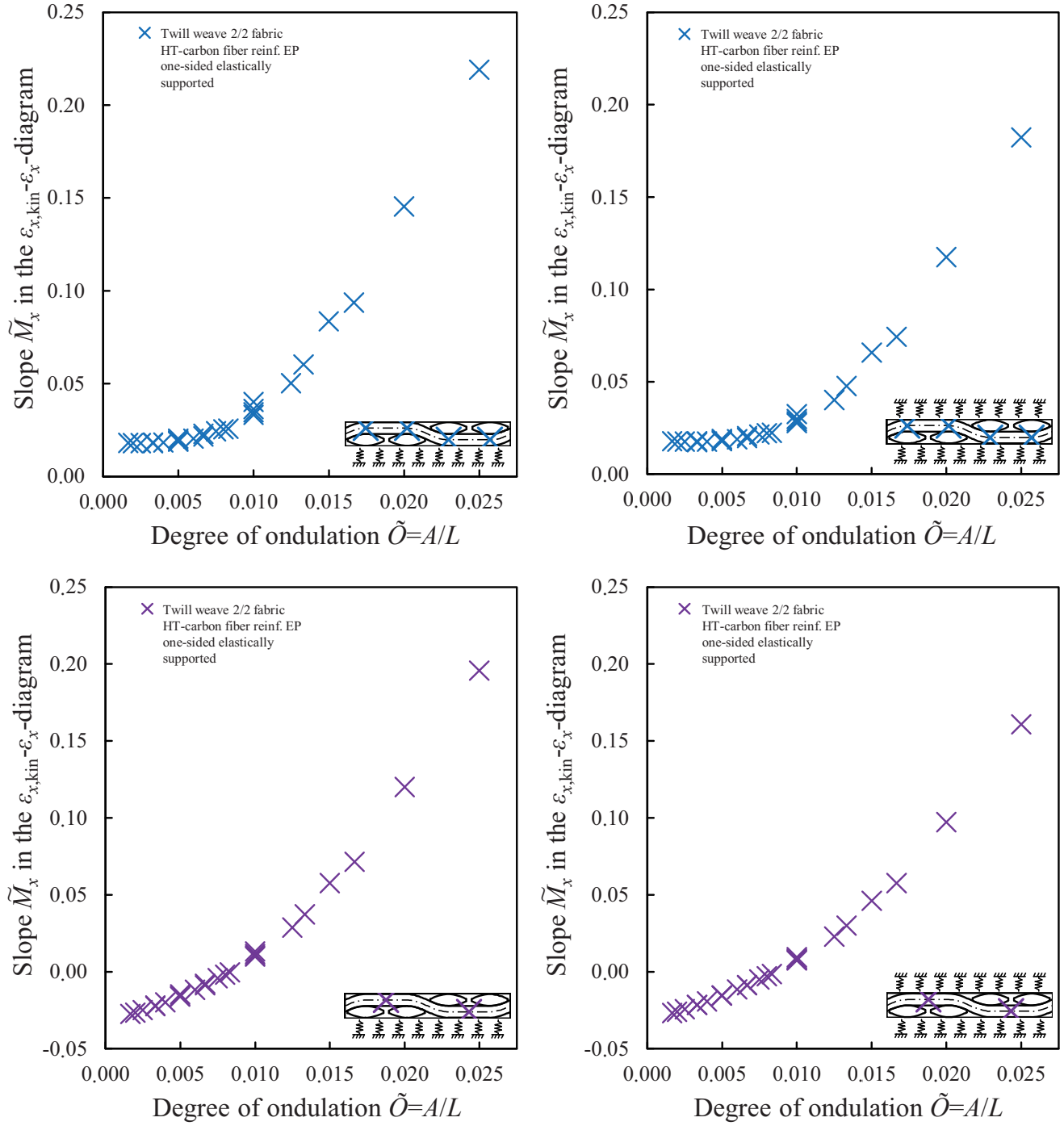

Fig. 9. Sensitivity $\tilde{M}_x\left(\tilde{O}\right)$ of the difference of longitudinal deformation $\varepsilon_{x,\mathrm{kin}}$ for twill-weave 2/2 fabric

For all evaluated positions regarding the difference longitudinal deformation $\varepsilon_{x,\mathrm{kin}}$ (12), as illustrated in Figure 9, there is an increasing sensitivity. Additionally, it is possible to imply a quadratic correlation. The sensitivity is always positive in case of the transition of ondulated and horizontal regions. In contrast the sensitivity in the middle of the horizontal regions is partially even negative. Generally the evaluated positions in case of the one-sided elastic support once again show a higher sensitivity to the mesomechanic kinematic as in case of the two-sided elastic support.

6. Discussion

Due to the geometric similar parameters and the identic structural mechanic material properties the results of the two kinds of fabrics are comparable to each other. Finally the limits of the carried out numerical investigations are described.

6.1. Limits of the model

The correlations are identified by simplifying presumptions. These are the ideal relation of the stiffnesses, the linear-elastic material model, the consideration of only two dimensions and an ideal mesomechanic geometry of balanced fabrics. They provide a description of the kinematic behaviour by trend, yet create at the same time limits of the model.

The different behaviour of fibre reinforced plastics under tensile and compression load, the quality of the intra- and interlaminar adhesion or other damages as imperfections influence the real material behaviour. They are not considered in the FE analyses.

In previous publications mesomechanic kinematic correlations in fabrics are generally considered nonlinear. Investigations of dry fabrics without matrix system under uniaxial and biaxial loading as well as under shear loading, as described by Badel, Vidal-Sallé and Boisse 2007 [14], Ballhause 2007 [11], Hivet and Boisse 2008 [15] as well as by Hivet and Duong 2010 [18], yield a different, likewise nonlinear correlation. Positive deformations at first cause a flattening of the ondulated rovings and thereby a reduction of the thickness. Under further application of positive deformations the smoothing or flattening of the loaded yarns even causes a rising of the transversal yarns. This results in an increase of the thickness of the fabric instead of a decrease, that is expected due to Poisson effects.

Because the considered ranges of deformation are relatively small, a linear-elastic material behaviour is presumed. It is concluded, that the identified correlations correctly describe the kinematic of fabrics in a mesomechanic scale. Larger ranges of deformations go beyond the limits of linearity, and cause non-linear effects.

6.2. Influence of the position of the single layer

The case-by-case analysis always yields higher sensitivities for the one-sided elastic support than for the two-sided one, where transversal deformation effects are inhibited. Thus, the higher sensitivities for one-sided elastic support $\tilde{M}_{\mathrm{o}}$ are related to the smaller ones for two-sided one $\tilde{M}_{\mathrm{t}}$. The results $\tilde{M}_{\mathrm{o}} / \tilde{M}_{\mathrm{t}}$ are plotted over the degree of ondulation $\tilde{O}$, for a plain-weave fabric in Figure 10 and for a twill-weave 2/2 fabric in Figure 11.

Plain-weave fabric

In case of $\tilde{M}_{y}\left(\tilde{O}\right)$, i. e. the kinematic parts $\varepsilon_{y,\mathrm{kin}}$ (9), as illustrated in Figure 10 left, the model with a one-sided elastic support shows a 1.8 times higher sensitivity as the model with a two-sided one. The relation at smaller degrees of ondulation $\tilde{O}$ is partially slightly higher. From $\tilde{O} \geq 0.02$ the relation slightly increases. In case of $\tilde{M}_{x}\left(\tilde{O}\right)$, i. e. the difference of longitudinal deformation $\varepsilon_{x,\mathrm{kin}}$ (12), as illustrated in Figure 10 right, the model with a one-sided elastic support only slightly differs from the one with a two-sided support. The relation is almost constant approximately 1. Up to $\tilde{O} \leq 0.02$ it is almost exactly 1, whereas for increasing it slightly increases up to 1.2, tops.

Twill-weave 2/2 fabric

In case of $\tilde{M}_{y}\left(\tilde{O}\right)$, i.e. the kinematic parts $\varepsilon_{y,\mathrm{kin}}$ (9), the model with a one-sided elastic support shows a 1.6 times higher sensitivity as the model with a two-sided one. The relation at the positions of transition, as illustrated in Figure 11 top left, at $\tilde{O}$ <0.01 is partially distinctly lower and increases to the value of 1.6. From $\tilde{O} \geq 0.01$ the relation remains constant at 1.6. In case of the evaluated positions in the middle, as illustrated in Figure 11 bottom left, there is a higher sensitivity to the mesomechanic kinematic in case of the one-sided elastic support.

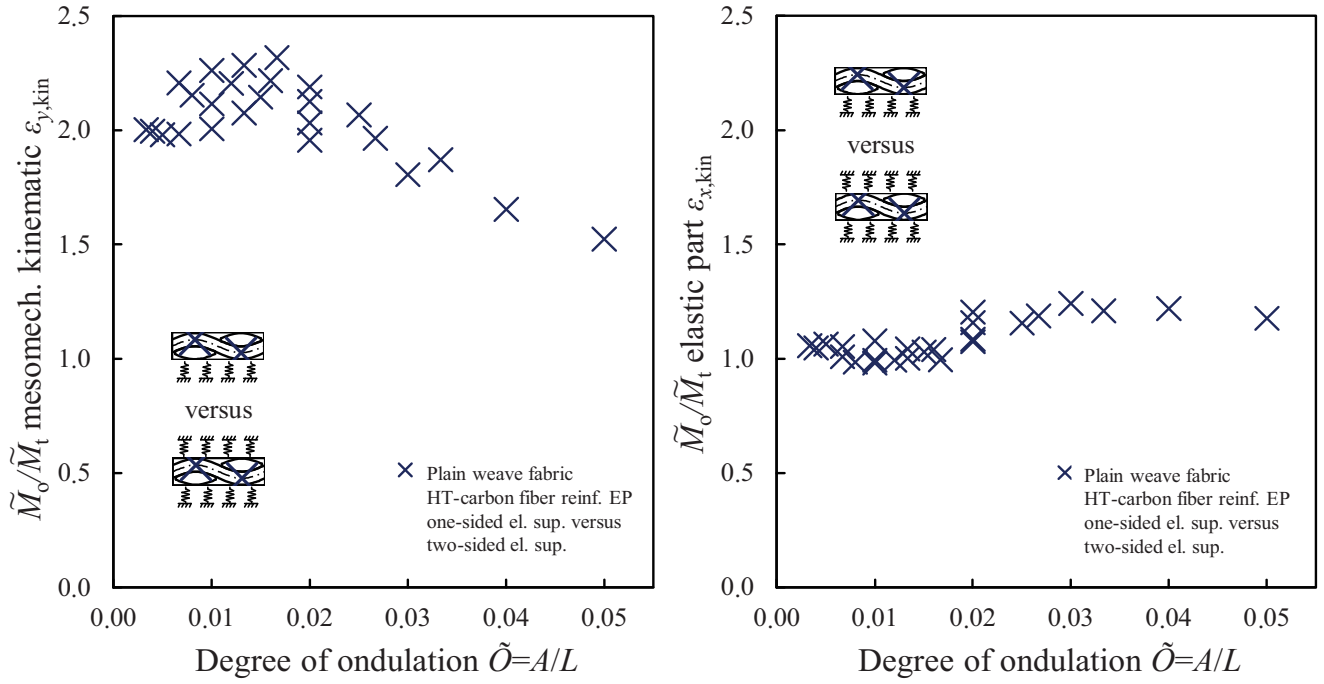

Fig. 10. Relations of the sensitivity $\tilde{M}_o / \tilde{M}_t$ for plain-weave fabric

At smaller degrees of ondulation the relation shows only a slight increasing. Not until $\tilde{O} > 0.01$ there is a distinct tendency to higher values.

In case of $\tilde{M}_x(\tilde{O})$, i.e. the difference of longitudinal deformation $\varepsilon_{x,kin}$ (12), at the positions of transition the different boundary conditions nearly have no influence, as illustrated in Figure 11 top right. The relation is almost constant about approximately 1, what represents the former mentioned similarity. It slightly increases up to $\tilde{O} \leq 0.01$, and does not change significantly for increasing degrees of ondulation.

In case of the evaluated positions in the middle, as illustrated in Figure 11 bottom right, there is once more no significant difference regarding the two cases of elastic support. The relation is almost approximately 1, too. At $\tilde{O}$=0.0067…0.01 there is a singularity, that initially yields very small and finally very high values. Yet, the general behaviour of the elastic part at the positions in the middle corresponds to the one of the positions at the transition. Correspondingly the positions at the transition at one-sided elastic support nearly do not differ from them at two-sided elastic support, so that the relation up to $\tilde{O}$=0.00667 is almost constant about approximately 1. Not until $\tilde{O} > 0.01$ the relation is nearly 1.2, and does not change significantly for increasing degrees of ondulation.

Comparison

For both the plain-weave and the twill-weave 2/2 fabric of carbon fibre reinforced epoxy the relations of the kinematic parts $\varepsilon_{y,kin}$ and the difference of the longitudinal deformation $\varepsilon_{x,kin}$ show, that the model for the one-sided elastic support always yields higher values than for the two-sided one. The relations of the kinematic $\varepsilon_{y,kin}$ are distinctly higher than the ones of the difference of the longitudinal deformation $\varepsilon_{x,kin}$.

The reduction of the relations of the kinematic parts $\varepsilon_{y,kin}$ for increasing degrees of ondulation, as illustrated in Figure 10 left and 11 top left, can be lead back to the increasing sensitivity at two-sided elastic support. Despite of the two-sided elastic support, that generally inhibits deformation, the effect of the mesomechanic kinematic increases for increasing degrees of ondulation. In contrast the geometric deviation at smaller degrees of ondulation is still too small, so that the two-sided elastic support distinctly counteracts the mesomechanic kinematic, and the model follows the behaviour of a 0°-unidirectionally reinforced sequence.

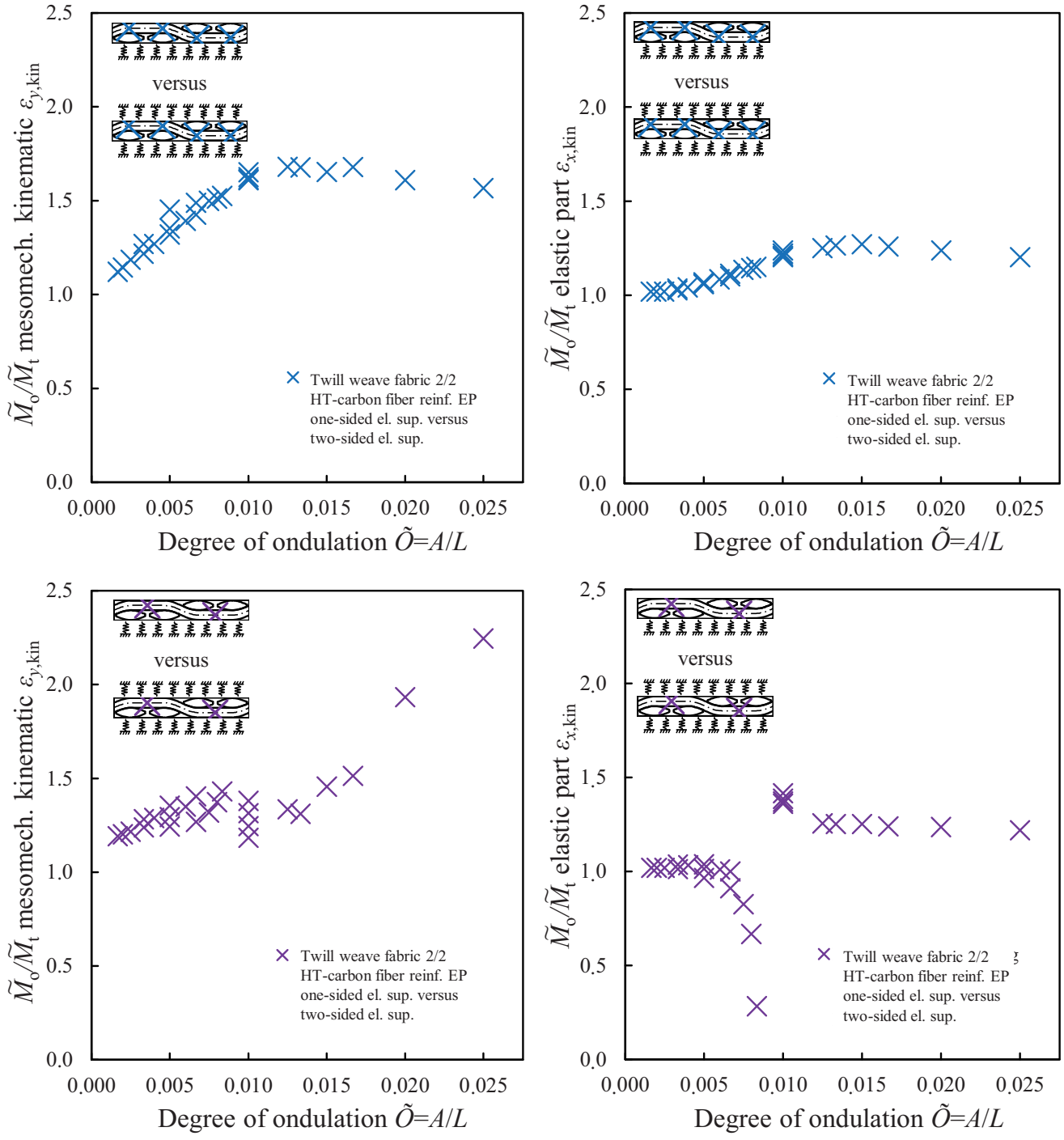

Fig. 11. Relations of the sensitivity $\tilde{M}_o / \tilde{M}_t$ for twill-weave 2/2 fabric

Only the kinematic parts $\varepsilon_{y,kin}$ at the positions in the middle of a twill-weave 2/2 fabric, as illustrated in Figure 11 bottom left, show a different behaviour. The tendency of increasing relations at very high degrees of ondulation once again indicates a very high sensitivity to the mesomechanic kinematic. This is

lead back to the modelling of plain representative sequences.

The horizontal unidirectionally reinforced regions adjoin pure matrix without reinforcement. In contrast the positions of evaluations at the transition or the extrema always directly adjoin a fill yarn. The different local transversal deformation behaviour contributes to the mesomechanic kinematic at the corresponding positions. The positions in the middle of a twill-weave 2/2 fabric have to be considered as an exception. Another reason in combination with the low sensitivity to the degree of ondulation is, that the unidirectionally reinforced warp yarn is not ondulated at the positions in the middle, so that there is no geometric deviation of the flow of forces.

The sensitivities of the difference of longitudinal deformation $\varepsilon_{x,\mathrm{kin}}$ yield nearly the same contribution at every position. The slight increase with increasing degree of ondulation, as illustrated in Figures 10 right and 11 right at the corresponding positions, acts analogue to the kinematic part of the increasing sensitivity at two-sided elastic support. The increasing effect of the mesomechanic kinematic at decreasing degrees of ondulation causes an increase of the elastic part. The reason is a generally inhibited deformation behaviour in case of the two-sided elastic support. Here, too, the mechanic behaviour of the representative sequence at smaller degrees of ondulation distinctly follows the behaviour of a 0°-unidirectionally reinforced sequence. There is only a slight geometric deviation of the ondulated roving. This behaviour does not depend neither on the kind of fabric construction nor on the different boundary conditions of a fabric in a laminate.

7. Summary and outlook

The summarized results and the concluded causal correlations obtained on the mesomechanic scale are given. Finally an outlook is described.

7.1. Summary

The identified correlations in the numerical investigations definitely prove the acting of a mesomechanic kinematic due to geometric constraints in plain-weave and twill-weave 2/2 fabrics. For a characterization of the mesomechanic geometric parameters the degree of ondulation $\tilde{O}=A/L$ (4) as a specific, non-dimensional value is introduced. The verification of correlation and causality between the mesomechanic kinematic and the degree of ondulation justifies its introduction. As it describes the geometric relations of fabrics in a mesomechanic scale, it is considered reasonable and productive.

The numerical investigations are carried out for balanced plain weave and twill-weave 2/2 fabric constructions of HT carbon fibre reinforced epoxy. The variation of the two geometric parameters in five substeps each provides 25 different degrees of ondulation for every fabric construction. This yields 50 geometries of the plain representative sequence. Two basically different boundary conditions of a fabric, i.e. one-sided and two-sided elastically supported, in total provides 100 FE models. The results (kinematic part $\varepsilon_{y,\mathrm{kin}}$ (9) and difference of longitudinal deformations $\varepsilon_{x,\mathrm{kin}}$ (12)) prove and verify the acting mechanical principle at the positions of evaluation.

Within the limits of the validity of the numerical model there is a direct linear coupling between the applied longitudinal deformations and the mesomechanic kinematic. In the FE calculations the elastic transversal deformation due to Poisson effects is separated and corrected, in order to obtain the purely mesomechanic kinematic.

7.2. Outlook

More parameters can be varied in the FE calculations. Correlations regarding loading and displacements as well as deformations are relevant. A parameter identification of the mesomechanic kinematic regarding the correlations of load and displacement provides the basis for the identification of the influence of the reinforcement fibre (glass, aramid, basalt compared to carbon) and of the fabric construction (other twill weave, satin weave (balanced and unbalanced) compared to plain-weave and twill-weave 2/2) on the mesomechanic material behaviour of fabrics. The consideration of a linear visco-elastic material instead of a linear-elastic one, and of the sensitivity of the material behaviour on the kind of deformation (tension or compression) provide another expansion of the limits of the model conceptions. The expansion to the third direction as the width of the structure, so that representative volume elements (RVEs) are considered, provides a further extension of surface structures.

References

[1] N.K. Naik, P.S. Shembekar, Elastic Behavior of Woven Fabric Composites: I-Lamina Analysis, Journal of Composite Materials 26/15 (1992) 2196-2225, DOI: https://doi.org/10.1177/002199839202601502.

[2] S.K. Mital, L.N. Murthy, C.C. Chamis, Simplified Micromechanics of Plain Weave Composites, NASA Technical Memorandum 107165, 1996, 1-12.

[3] H. Guan, Micromechanical analysis of viscoelastic damping in woven fabric-reinforced polymer matrix composites, PhD Thesis, Wayne State University, Detroit (Michigan, USA), 1997, Paper AAI9725829, http://digitalcommons.wayne.edu/dissertations/AAI9725829.

[4] J.H. Byun, The analytical characterization of 2-D braided textile composites, Composites Science and Technology 60/5 (2000) 705-716, DOI: https://doi.org/10.1016/S0266-3538(99)00173-6.

[5] Z.M. Huang, The mechanical properties of composites reinforced with woven and braided fabrics, Composites Science and Technology 60/4 (2000) 479-498, DOI: https://doi.org/10.1016/S0266-3538(99)00148-7.

[6] H. Guan, R.F. Gibson, Micromechanic Models for Damping in Woven Fabric-Reinforced Polymer Matrix Composites, Journal of Composite Materials 35/16 (2001) 1417-1434, DOI: https://doi.org/10.1106/NEJY-H235-66RD-G635.

[7] A. Tabiei, W. Yi, Comparative study of predictive methods for woven fabric composite elastic properties, Composite Structures 58/1 (2002) 149-164, DOI: 10.1016/S0263-8223(02)00028-4.

[8] B.H. Le Page, F.J. Guild, S.L. Ogin, P.A. Smith, Finite element simulation of woven fabric composites, Composites: Part A 35/7-8 (2004) 861-872, DOI: 10.1016/j.compositesa.2004.01.017.

[9] B. Wielage, T. Müller, T. Lampke, U. Richter, E. Kieselstein, G. Leonhardt, Simulation der elastischen Eigenschaften gewebeverstärkter Verbundwerkstoffe unter Berücksichtigung der Mikrostruktur, in: M. Schlimmer (Ed.), Proceedings of the 15th Symposium Verbundwerkstoffe und Werkstoffverbunde, Kassel, Germany, Weinheim, Wiley VCH Verlag, 2005, 441-446, http://www.dgm.de/download/tg/706/706_77.pdf, (in German).

[10] E.J. Barbero, J. Trovillion, J.A. Mayugo, K.K. Sikkil, Finite Element Modeling of Plain Weave Fabrics from Photomicrograph Measurements, Composite Structures 73/1 (2006) 41-52, DOI: https://doi.org/10.1016/j.compstruct.2005.01.030.

[11] D. Ballhause, Diskrete Modellierung des Verformungs- und Versagensverhaltens von Gewebemembranen, PhD Thesis, University of Stuttgart, Germany, 2007 (in German).

[12] T. Matsuda, Y. Nimiya, N. Ohno, M. Tokuda, Elastic-viscoplastic behavior of plain-woven GFRP laminates: Homogenization using a reduced domain of anlysis, Composite Structures 79/4 (2007) 493-500, DOI: https://doi.org/10.1016/j.compstruct.2006.02.008.

[13] Y. Nakanishi, K. Matsumoto, M. Zako, Y. Yamada, Finite element analysis of vibration damping for woven fabric composites, Key Engineering Materials 334-335 (2007) 213-216, DOI: https://doi.org/10.4028/www.scientific.net/KEM.334-335.213.

[14] P. Badel, E. Vidal-Sallé, P. Boisse, Computational determination of in-plane shear mechanic behaviour of textile composite reinforcements, Computational Material Science 40/4 (2007) 439-448, DOI: https://doi.org/10.1016/j.commatsci.2007.01.022.

[15] G. Hivet, P. Boisse, Consistent mesoscopic mechanical behavior model for woven composite reinforcements in biaxial tension, Composites Part B: Engineering 39/2 (2008) 345-361, DOI: https://doi.org/10.1016/j.compositesb.2007.01.011.

[16] A. El Mahi, M. Assarar, Y. Sefrani, J.-M. Berthelot, Damping analysis of orthotropic composite materials and laminates, Composites Part B: Engineering 39/7-8 (2008) 1069-1076, DOI: https://doi.org/10.1016/j.compositesb.2008.05.003.

[17] P. Szablewski, Sinusoidal Model of Fiber-reinforced Plastic Composite, Journal of Industrial Textiles 38/4 (2009) 277-288, DOI:10.1177/1528083708098914.

[18] G. Hivet, A.V. Duong, A contribution to the analysis of the intrinsic shear behavior of fabrics, Journal of Composite Materials 45/6 (2010) 695-716, DOI: https://doi.org/10.1177/0021998310382315.

[19] M. Ansar, W. Xinwei, Z. Chouwei, Modeling strategies of 3D woven composites – A review, Composite Structures 93/8 (2011) 1947-1963, DOI: https://doi.org/10.1016/j.compstruct.2011.03.010.

[20] J. Kreikmeier, D. Chrupalla, I.A. Khattab, D.S. Krause, Experimentelle und numerische Untersuchungen von CFK mit herstellungsbedingten Fehlstellen, in: Proceedings of the 10. Magdeburger Maschinenbau-Tage, Magdeburg, Germany, 2011 (in German).

[21] P. Ottawa, M. Romano, I. Ehrlich, M. Wagner, N. Gebbeken, The influence of ondulation in fabric reinforced composites on dynamic properties in a mesoscopic scale in composites reinforced with fabrics on the damping behaviour, Proceedings of the 11th LS-DYNA Forum, Ulm, Germany, 2012, 171-172, http://www.dynamore.de/de/download/papers/ls-dyna-forum-2012.

[22] M. Romano, I. Ehrlich, N. Gebbeken, Parametric characterization of a mesomechanic kinematic caused by ondulation in fabric reinforced composites: analytical and numerical investigations, Fracture and Structural Integrity (FIS) 11/39 (2017) 226-247, http://www.fracturae.com/index.php/fis/article/view/IGF-ESIS.39.22/1860.

[23] M. Romano, M. Micklitz, F. Olbrich, R. Bierl, I. Ehrlich, N. Gebbeken, Experimental investigation of damping properties of unidirectionally and fabric reinforced plastics by the free decay method, Journal of Achievements in Materials and Manufacturing Engineering 63/2 (2014) 65-80, http://www.journalamme.org/vol63_2/6323.pdf.

[24] M. Romano, M. Micklitz, F. Olbrich, R. Bierl, I. Ehrlich, N. Gebbeken, Experimental investigation of damping properties of unidirectionally and fabric reinforced plastics by the free decay method, Proceedings of the 15th International Materials Symposium "IMSP'2014", Denizli, Turkey, 2014, 665-679, http://imsp.pau.edu.tr/IMSP2014_Proceedings_Final_security.pdf.

[25] M. Romano, Charakterisierung von gewebe-verstärkten Einzellagen aus kohlenstofffaser-verstärktem Kunststoff (CFK) mit Hilfe einer mesomechanischen Kinematik sowie struktur-dynamischen Versuchen, in: I. Ehrlich, U. Briem (Eds.), Schriftenreihe der OTH Regensburg, Aachen/Regensburg, Germany, Shaker Verlag, 2017, DOI: 10.2370/9783844051773 (in German).

[26] I.N. Bronstein, K.A. Semendajew, Taschenbuch der Mathematik, Seventh Edition, Frankfurt am Main, Germany, Verlag Harri Deutsch, 2008 (in German).

[27] L. Papula, Mathematische Formelsammlung für Ingenieure und Naturwissenschaftler, Ninth Edition, Wiesbaden, Germany, Vieweg+Teubner, 2006, (in German).

[28] F. Büsching, Combined Dispersion and Reflection Effects at Sloping Structures, Proceedings of the International Conference on Port and Marine R&D and Technology "ICPMRDT", Vol. I, Singapore, 2001, 410-418.

[29] K. Stellbrink, Micromechanics of Composites, München/Wien, Germany/Austria, Hanser-Verlag, 1996 (in German).

[30] ANSYS, ANSYS 14.0 Help, Helpsystem of ANSYS Workbench Version 14.0.1, SAS IP Inc., Canonsburg, Pennsylvania, USA, 2011.

[31] R.M. Jones, Mechanics of composite materials, Second Edition, Philadelphia, USA, Taylor & Francis, 1999.

[32] K. Moser, Faser-Kunststoff-Verbund – Entwurfs- und Berechnungsgrundlagen, Düsseldorf, Germany, VDI-Verlag, 1992 (in German).

[33] H. Schürmann, Konstruieren mit Faser-Kunststoff-Verbunden, Berlin/Heidelberg/New York, Springer-Verlag, 2005 (in German).

[34] C.C. Chamis, Simplified Composite Micromechanics Equations for Hygral, Thermal and Mechanical Properties, in: NASA Technical Memorandum 83320, Prepared for the Thirty-eight Annual Conference of the Society on the Plastics Industry (SPI), Houston, Texas, USA, 7-11 February, 1-10, Houston, Reinforced Plastics/Composites Institute.

[35] C.C. Chamis, Simplified Composite Micromechanics Equations for Hygral, Thermal and Mechanical Properties, SAMPE Quarterly 2 (1984) 14-23.

[36] S.W. Tsai, H.T. Hahn, Introduction to Composite Materials, Lancaster, USA, Technomic Publishing, 1980.

[37] R.L. Foye, The transverse poisson's ratio of composites, Journal of Composites Materials 6/2 (1972) 293-295, DOI: https://doi.org/10.1177/002199837200600209.

[38] E.J. Barbero, Introduction to Composite Materials Design, Second Edition, Boca Raton/London/New York, CRC Press – Taylor & Francis Group, 2011.

[39] E.J. Barbero, R. Luciano, Micromechanics Formulas for the Relaxation Tensor of linear Viscoelastic Composites with Transversely Isotropic Fibers, International Journal of Solids and Structures 32/13 (1995) 1859-1872, DOI: https://doi.org/10.1016/0020-7683(94)00233-M.

[40] P. Valentino, F. Furgiuele, M. Romano, I. Ehrlich, N. Gebbeken, Mechanical characterization of basalt fibre reinforced plastic with different fabric reinforcements – Tensile tests and FE-calculations with representative volume elements (RVEs), in: F. Iacoviello, G. Risitano, L. Susmel (Eds.), Acta Fracturae – XXII Convegno Nazionale IGF (Italiano Gruppo Frattura), Roma, Italy, 1-3 July 2013, 231-

244, Roma, Italiano Gruppo Frattura (IGF), http://www.gruppofrattura.it/ocs/index.php/cigf/IGF22/paper/view/10914/10241.

[41] P. Valentino, E. Sgambitterra, F. Furgiuele, M. Romano, I. Ehrlich, N. Gebbeken, Mechanical characterization of basalt woven fabric composites: numerical and experimental investigation, Fracture and Structural Integrity (FIS) 28/8 (2014) 1-11, http://www.gruppofrattura.it/ors/index.php/fis/article/view/1229/1182, DOI: 10.3221/IGF-ESIS.28.01.